

Learning by Sorting: Self-supervised Learning with Group Ordering Constraints

Nina Shvetsova^{1,3} Felix Petersen² Anna Kukleva³ Bernt Schiele³ Hilde Kuehne^{1,4}

¹Goethe University Frankfurt, ²Stanford University, ³Max-Planck-Institute for Informatics, ⁴MIT-IBM Watson AI Lab

shvetsov@uni-frankfurt.de

Abstract

Contrastive learning has become a prominent ingredient in learning representations from unlabeled data. However, existing methods primarily consider pairwise relations. This paper proposes a new approach towards self-supervised contrastive learning based on Group Ordering Constraints (GroCo). The GroCo loss leverages the idea of comparing groups of positive and negative images instead of pairs of images. Building on the recent success of differentiable sorting algorithms, group ordering constraints enforce that the distances of all positive samples (a positive group) are smaller than the distances of all negative images (a negative group); thus, enforcing positive samples to gather around an anchor. This leads to a more holistic optimization of the local neighborhoods. We evaluate the proposed setting on a suite of competitive self-supervised learning benchmarks and show that our method is not only competitive to current methods in the case of linear probing but also leads to higher consistency in local representations, as can be seen from a significantly improved k -NN performance across all benchmarks.

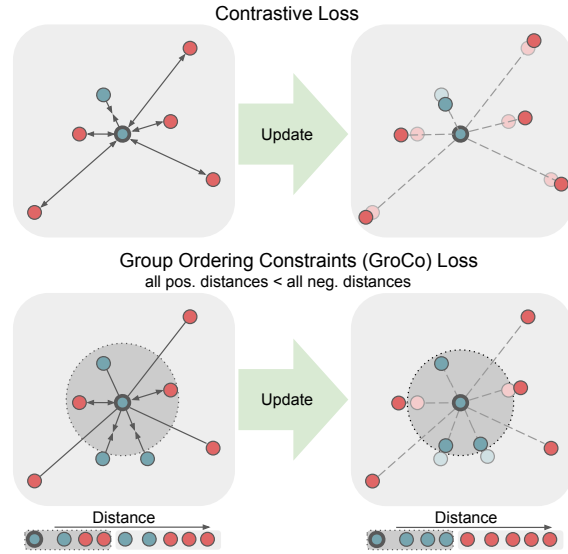


Figure 1. Pairwise contrastive loss compared to the proposed group ordering constraints loss: While pairwise loss only considers pairwise distances, groupwise sorting allows us to enforce that a group of positive samples is closer to the anchor than a group of negative ones and, thus, to improve the representation of the local neighborhood.

1. Introduction

Self-supervised learning has become a topic of growing interest over the last years as it allows models to learn representations from large-scale data without any need for annotation. Recently, self-supervised contrastive methods [3, 10, 17, 26, 51, 56] notably narrowed the gap to the supervised learning performance. These methods rely on the concept of the pairwise contrastive loss, which is based on the idea that an image, serving as anchor, and an augmentation of the same image, a so-called positive pair, should be close to each other in a projection space, while a pair made up of an anchor image and a different image, a so-called negative pair, should be far away from each other. This concept of bringing positive pairs in embedding space closer together was further extended in various frameworks, such

as BYOL [23], SwAV [8], and many more [4, 9, 13, 19, 58].

However, the idea of the pairwise contrastive loss is limited by the fact that it only considers individual positive pairs. This means that it can not align the embedding space based on more than two positive data points. Several attempts have been made to address this issue, e.g., combining the contrastive idea with concepts based on local neighborhoods, such as clustering as in the case of SwAV [8], or minimizing distances between multiple positives pairs for the same instance together as in the case of Whitening [19]. Another limitation of the contrastive loss is that it requires a large number of negatives in order to be effective [10]. Some methods tackle this issue by leveraging a large batch size [10], memory banks [26], or negative mining [52]. However, here, a drawback is that, as the embedding space is optimized with respect to all negatives, even

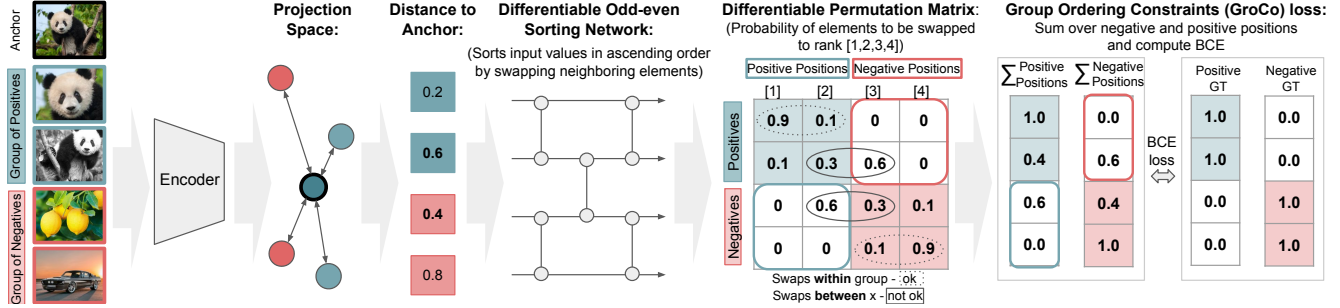


Figure 2. Overview of the proposed group ordering constraints loss: We first compute the distance of groups of positive as well as negative samples with respect to an anchor. The distances are sorted via a differentiable odd-even-sorting network in non-descending order, computing the *swapping probability for samples*. The result is a differentiable permutation matrix, in which the row values can be thought of as the probabilities of sorting the elements into the corresponding positions. We can ignore swap operations within groups, and only need to consider swapping operations between groups. We, therefore, sum over the positive and negative columns of the permutation matrix and compute the BCE between the row-wise entries and the expected ground truth.

negatives that are far away from the anchor will contribute to the optimization of the representation. Other methods were proposed to address this issue, such as hard negative selection by controlling the hardness of examples [47] or negative selection by sparse support vectors [50]. Yet, these methods still require manual selection of the hardness level [47] or incur an additional optimization cost [50].

In this paper, we propose a novel approach to address those points by shifting away from the concept of a pairwise contrastive loss and instead propose to train the network based on Group Ordering Constraints (GroCo)—namely, the idea that the group of multiple positives should be closer to an anchor image than any negative from the group of negatives. We illustrate this idea and comparison with the pairwise contrastive loss in Figure 1. With group constraints, we do not treat positive and negative pairs individually, as in contrastive loss, but rather as groups, and effectively constrain only those elements that are placed in the group overlap area with respect to the distance to the anchor point.

To enforce the group ordering constraints in the projection space, we propose the idea of *learning by sorting*: we suggest sorting positives and negatives by distance to the anchor image in a differentiable way and swapping them if they are in the wrong order. To create an end-to-end training pipeline, we leverage recent advances in differentiable sorting [16, 24, 41, 42]. Specifically, we utilize a differentiable sorting algorithm to obtain a differentiable permutation matrix for sorting a list of distances to the positive and negative images, as shown in Figure 2. If we would know the full ground truth orderings among positives and negatives, such as which positive sample should be closer to the anchor than another positive sample, we could create a ground truth permutation matrix, and calculate how much the predicted permutation matrix would deviate from the ground truth one [16, 24, 41, 42]. Since this assumption is not given in practice and we do not know the ground truth distance ordering within the positive or the negative

groups, we propose the GroCo loss, a relaxed formulation of the original sorting supervision that captures how many negative elements appear in the positive positions and vice versa. Compared to the pairwise contrastive loss, the resulting group ordering focuses on *optimizing the local neighborhood* around an anchor image, rather than optimizing all data points at once. Moreover, without any additional modifications, our group ordering loss directly focuses on the strongest positive and negative examples.

To show the capabilities of the proposed approach, we evaluate it on a suite of competitive self-supervised learning benchmarks, namely in the context of linear probing, k -NN classification, as well as image retrieval. Our evaluation demonstrates that models trained via group ordering constraints obtain competitive performance in linear evaluation compared to other contrastive learning frameworks, some of them even trained with significantly larger batch sizes and/or an additional teacher network. Further, we demonstrate the superior ability of the proposed method in the context of shaping local neighborhoods by evaluating the nearest neighbor classification capabilities by outperforming any other state-of-the-art method on this task.

We summarize the contributions of this work as follows¹:

- We propose a new concept for self-supervised representation learning based on learning by sorting.
- We leverage recently proposed differentiable sorting methods to derive the contrastive group ordering constraints (GroCo) loss.
- We demonstrate that the proposed method achieves competitive performance in linear separability of embeddings and is especially suitable to model the local neighborhoods and outperforms current top-level state-of-the-art frameworks on a wide range of nearest-neighbor tasks.

¹The code will be made publicly available.

2. Related Work

2.1. Self-supervised Representation Learning

Self-supervised learning aims to learn a robust representation from data without human annotation. Various learning objectives were developed for self-supervised learning from images including image colorization [60], inpainting [40], puzzle solving [37], and rotation prediction [22].

Over the last years, methods [8, 10, 13, 23, 26] that enforce the model to be robust to different image distortions achieved great performance improvements in self-supervised learning. Such methods generally rely on sampling two augmented views of the image—a positive pair—and minimize the distance between those in the embedding space. Contrastive methods [10–12, 26] are a great example of those approaches. To prevent the model from learning a trivial solution for any input, contrastive methods also introduce the concept of a negative pair, i.e., two different image, and *contrast* positive pairs against negative pairs. The InfoNCE loss, which is often referred to as a contrastive loss, is the most prominent method in many self-supervised learning scenarios [1, 10, 26, 46]. Earlier contrastive methods relied on the triplet loss [49], which considers one positive and one negative example for the anchor image. In contrastive learning, many components and extensions have been investigated: data augmentation strategies [10, 54], projection head design [11], hard negative sampling [47], increasing the richness of positives with nearest neighbours [17], or mitigating effect of false negatives [28]. In this work, we propose a novel contrastive method—learning by sorting—which features properties not inherent to other contrastive learning methods: we primarily consider those positives and negatives that are placed (sorted) incorrectly in the embedding space, thereby implicitly considering the strongest positive and negative examples.

There are also methods [13, 23] that do not rely on negatives and only maximize agreement between positive views. Such methods prevent collapsing of the representation space by using asymmetric architectures applied to different views [13, 23], an additional teacher network [9, 23], stop gradient [9, 13, 23], feature whitening [19], or information maximization [4, 58]. Another set of methods [2, 7, 8] utilizes clustering of the latent embeddings. However, so far, methods mostly rely on similarity maximization between only two sampled views. SwAV [8] also considered sampling more augmentations in a multi-crop setting, where two full-size augmented images are sampled together with several smaller crops, and Whitening [19] utilized more full-resolution samples. However, even in these cases, the loss was still computed by considering pairs of views independently. In contrast, we propose optimizing the embedding space based on *group ordering constraints*.

2.2. Differentiable Sorting and Ranking

Differentiable sorting and ranking methods provide a pipeline that allows training neural networks with ordering supervision in an end-to-end fashion with gradient descent [5, 16, 24, 41, 42, 44]. The sorting operator can be seen as a function returning a permutation matrix that indicates the permutation necessary to sort the sequence of values (the matrix that multiplied with a input vector returns a sorted output vector.) In this context, differentiable sorting refers to relaxing the (hard) permutation matrix to a differentiable permutation matrix via continuous relaxations. The differentiable permutation matrix for a given sequence of values, which could, e.g., be scores predicted by a neural network, can then be used to compute the loss by comparison to a ground truth permutation matrix. Recently, multiple methods for relaxing the permutation matrix have been proposed, including an argsort approximation by unimodal row-stochastic matrices [24, 44], a formulation of entropy-regularized optimal transport [16], as well as networks of differentiable swap operations (differentiable sorting networks) [41, 42]. The latter method composes the full permutation matrix as a product of permutation matrices that arise from comparing only two elements at a time (usually neighbors) and either swapping them or not swapping them. Inspired by the idea of swapping the neighboring elements in the sequence, our approach learns representations by comparing neighboring elements in the embedding space.

In terms of applications, differentiable sorting has been leveraged in various contexts, including recommender systems [33], image patch selection [15], selection experts in multi-task learning [25], and attention mechanisms [59]. To the best of our knowledge, the proposed method is the first work to leverage ordering supervision for self-supervised learning of visual representations.

3. Method

Given a dataset of images $\{x_i\}_{i=1}^M \subseteq \mathcal{X}$, our goal is to learn an encoder $g : \mathcal{X} \rightarrow \mathbb{R}^d$ that extracts image representations that later might be used for downstream tasks.

3.1. Training Pipeline

Similar to other contrastive methods, our approach considers several augmented views of the same image as positive examples, which should be close together in an embedding space, and different images as negative examples, which should be apart in an embedding space. Our model starts from sampling mini-batches of B images and generates $m \geq 2$ randomly augmented views per each image, resulting in $m \cdot B$ data points. If $m = 2$ we are close to the original pairwise contrastive learning setup [4, 10, 13, 28, 58]. The augmented views are processed with the encoder network $g(\cdot)$, that extracts data representation vectors from views. Then, an MLP projection head $h(\cdot)$ maps represen-

tations to the latent space where distances between views are calculated. For each data point serving as an anchor x^a , we have $m - 1$ positive examples $\{x_i^p\}_{i=1}^{m-1}$ (which results in 1 positive example in the classical setup of $m = 2$) and $m \cdot (B - 1)$ negative examples $\{x_i^n\}_{i=1}^{m \cdot (B-1)}$. We use the cosine distance to measure the distance between data points: $d(x, y) = -\frac{x^\top y}{\|x\| \|y\|}$.

3.2. Group Ordering Constraints (GroCo)

In order to consider not only pairs of views but instead groups of multiple positives at once, we extend the contrastive loss to the idea that *the group of positives* should be closer to the anchor image than *the group of negatives* in the embedding space. This idea directly results in *group ordering constraints (GroCo)*. To simplify the notation, we denote the distance between data point x^a and its positive x_i^p and negative examples x_i^n as $d_i^p = d(x^a, x_i^p)$ and $d_i^n = d(x^a, x_i^n)$. If we assume that K positives x_1^p, \dots, x_K^p are ordered with respect to their distances to the anchor x^a as $d_1^p \leq \dots \leq d_K^p$ and N negatives x_1^n, \dots, x_N^n as $d_1^n \leq \dots \leq d_N^n$, then we define the *group ordering constraints* as

$$d_1^p \leq \dots \leq d_K^p < d_1^n \leq \dots \leq d_N^n. \quad (1)$$

As can be seen in Equation 1, all elements in the groups are considered in the constraints; however, for training, the relevant constraint is the (bold) $<$ in the center. This constraint differs from pairwise contrastive loss constraints, which 1) consider positives individually and 2) consider all negatives even if they are far away from the anchor and are thus less relevant. Our constraints also differ from the triplet loss, which considers only one positive and one negative example, while we are working with groups.

3.3. Learning by Sorting

Inspired by recent advances in differentiable sorting [41, 42], we design a loss that fulfills our group ordering constraints based on differentiable sorting. Our training procedure can be seen as sorting positives and negatives in the embedding space with respect to an anchor image and swapping them if they are in the incorrect order; therefore, we call the approach *learning by sorting*.

3.3.1 Differentiable Sorting Networks

In the following, we review the differentiable sorting algorithm called *differentiable sorting networks* [41] as it is a core element of our loss function. We note that “networks” in “sorting networks” is not related to the term “neural networks” and that a differentiable sorting network is a function with no trainable parameters. Sorting networks are a family of sorting algorithms from classic computer science literature [30]. An example of this is the odd-even sorting network. By relaxing the conditional swap operator to

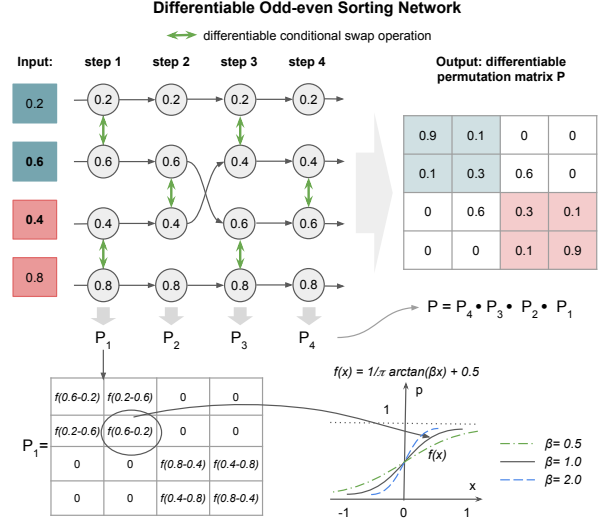


Figure 3. Overview of a differentiable sorting network with the odd-even sorting algorithm. The network compares neighboring elements that start from odd and even indices alternatively in each step and apply a differentiable swap operation if elements are in the wrong order. The conditional swap operations on each step s also define a differentiable permutation matrix P_s . The network output is a complete differentiable permutation matrix P , defined as the multiplication of matrices of each step.

a differentiable conditional swap, sorting networks can be made differentiable by relaxation to differentiable sorting networks [41].

We consider differentiable sorting networks based on the odd-even sorting network to sort an input sequence of $K + N$ elements in non-descending order as shown in Figure 3. The differentiable sorting network is defined as a composition of functions, where each function refers to one step of sorting, and where pairs of elements of the input sequence are compared and swapped if they are in the wrong order via a *conditional swap operation*. For the odd-even sorting network, the algorithm compares neighbored elements on odd and even indices alternatingly in each step, and requires $K + N$ steps to sort a given input sequence of length $K + N$.

The conditional swap operation for elements (d_i, d_j) where $i < j$ can be defined as $d'_i = \min(d_i, d_j)$, $d'_j = \max(d_i, d_j)$, and the differentiable relaxation [42] of this operation is defined as:

$$\begin{aligned} d'_i &= \text{softmin}(d_i, d_j) = d_i f(d_j - d_i) + d_j f(d_i - d_j) \\ d'_j &= \text{softmax}(d_i, d_j) = d_i f(d_i - d_j) + d_j f(d_j - d_i) \end{aligned} \quad (2)$$

where $f(x) = \frac{1}{\pi} \arctan(\beta x) + 0.5$ [42]. The hyperparameter $\beta > 0$ denotes an inverse temperature, and when $\beta \rightarrow \infty$ the relaxation converges to the discrete swap operation. The differentiable conditional swap operation for the elements (d_i, d_j) can be defined as a permutation matrix $P_{\text{swap}(d_i, d_j)} \in \mathbb{R}^{(K+N) \times (K+N)}$ is an identity matrix

except for entries $P_{ii}, P_{ij}, P_{jj}, P_{ji}$, which are defined as:

$$\begin{aligned} P_{ii} &= P_{jj} = f(d_j - d_i), \\ P_{ij} &= P_{ji} = f(d_i - d_j). \end{aligned} \quad (3)$$

The permutation matrix P_s for step s is the product of matrices corresponding to parallel (and thus independent) swap operations in this step $P_s = \prod_{i \in R} P_{\text{swap}(d_i, d_{i+1})}$, where R is the set of odd indices if s is odd and the set of even indices if s is even. The complete permutation matrix P is defined as $P = P_{K+N} \cdot \dots \cdot P_1$.

In the discrete case, each row of a permutation matrix has exactly one entry of 1, which indicate the position where the element that corresponds to this row should be placed. In the relaxed version, row values can be seen as a distribution over possible positions of the element [43]. For training with sorting supervision, where the correct order of input values is known, we can create a ground truth matrix Q and define the loss as $L = \frac{1}{(K+N)^2} \sum_{i,j} \text{BCE}(P_{ij}, Q_{ij})$ where BCE refers to binary cross-entropy.

3.3.2 GroCo Loss

If we would know the ground truth order of positives and negatives, we could create a ground truth permutation matrix and calculate a loss. However, as we rely on random augmentations, we do not know the ground truth order among positives and among negatives. Thus, we propose a solution to obtain a loss to fulfil our group ordering constraints.

Let us again assume that positives are ordered with respect to their distances to the anchor image as $d_1^p \leq \dots \leq d_K^p$ and negatives as $d_1^n \leq \dots \leq d_N^n$. As shown in Figure 3, we concatenate positive and negative distances in a list:

$$[d_1^p, \dots, d_K^p, d_1^n, \dots, d_N^n]. \quad (4)$$

Even though we have ordered elements in the positive and negative sub-list, we still don't know if the constraint $d_i^p < d_j^n$ is fulfilled for any $1 \leq i \leq K$ and $1 \leq j \leq N$.

Here, we apply a differentiable sorting network to the list and obtain a differentiable permutation matrix for sorting the list in non-descending order. Values in a permutation matrix row can be seen as probabilities to sort the corresponding element to the different positions, e.g., P_{11} would be the probability for assigning the first element in the list (d_1^p) to position 1, P_{12} to position 2, etc. Therefore, a sum of the first K elements in a row can be considered as a probability being sorted inside the first K elements. Thus, for a permutation matrix of size $(K+N) \times (K+N)$ the sum of the first K columns results in probabilities of being sorted in *positive places* and the later columns (from $K+1$ to $K+N$) in *negative places*. We define a loss that enforces

positives to be sorted in the positive places and negatives in the negatives places, as

$$\begin{aligned} L = \frac{1}{2(K+N)} \sum_{i=1}^{K+N} & \left(\text{BCE} \left(\sum_{k=1}^K P_{ik}, \mathbb{1}_{i \leq K} \right) + \right. \\ & \left. + \text{BCE} \left(\sum_{k=K+1}^{K+N} P_{ik}, \mathbb{1}_{i > K} \right) \right) \end{aligned} \quad (5)$$

where $\mathbb{1}$ is an indicator function.

As illustrated in Figure 2, our loss is a relaxation of the sorting supervision that considers only two types of swap operations: swap operations *within* the group of positive and negative samples, which should not contribute to the loss, and swap operations *between* the groups, which violate the positive-negative ordering assumption and which we want to use as the optimization criterion.

Role of Pre-ordering. Practically, we pre-order positives and negatives inside the groups in a non-differentiable way before inputting them into the differentiable sorting network. Though even without it, the loss will still contrast positives to negatives, we believe that pre-ordering fulfills the idea behind GroCO. When we input pre-ordered elements, the sorting network performs comparisons of neighboring elements swapping them if they are in the wrong order, or if everything is sorted correctly, comparing the strongest positive with the strongest negative. In this way, elements are considered as a group, and borders of the groups or their overlapping parts are used in the loss.

Number of Negatives. Since the only strongest negatives (that are sorted incorrectly) mostly participate in the computation of the loss function, we may use only top- N strongest negatives almost without losing any learning signal. We will show in the ablation study that $N = 10$ is enough.

Role of β . The inverse temperature β in differentiable swap operation corresponds to the degree of relaxation of the swap operation that converges to a discrete case when $\beta \rightarrow \infty$ (Figure 3). Therefore with lower β the swap operation is more "soft", which means that the variance in gradients is smaller, which is beneficial for optimization, but a relaxation error accumulated by steps is larger, and vice versa in the case of larger β . With higher β even a small difference between values results in a high probability for a swap or not swap operation, resulting in a smaller margin between the positive and negatives group. With lower β we push positive and negative groups further apart.

4. Experimental Evaluation

4.1. Implementation Details

Unless stated otherwise, we use the following setup for all of our experiments:

Augmentation. To create m augmented views per image (considering $m = 2, 3, 4$), we follow the DINO augmentation setup [9]. Since computational cost grows linearly with an increasing number of augmentations, we additionally considered the multi-crop augmentation strategy proposed in SwAV [8]. The idea is to sample low-resolution *local* views along with the standard 224×224 ones. We use $2 \times 224 + 6 \times 96$ scheme, where with two *global* 224×224 augmented views, we also sampled six *local* 96×96 views, giving eight views per image. In this case, we follow “*local-to-global*” correspondence idea [8, 9] and use only global views as positives for both local and global anchor images.

Model. To be consistent with previous works [8, 10, 13, 23] we use Resnet50 [27] as the encoder $g(\cdot)$ and an MLP block consisting of three fully connected layers with a size of 2048 and followed by a batch normalization layer [29] as the projection head $h(\cdot)$. All batch normalization layers except the last one are followed by a ReLU activation. The dimensionality of the representation space and the latent space are both 2048 as in [13]. We also adopt the stop gradient operation, which is widely used in different self-supervised learning methods [9, 10, 23]; specifically, we perform stop gradient during distance computation $d(x^a, x_i^b) = d(x^a, \text{stop_grad}(x_i^b))$. While we found that it is not strictly necessary for a successful training of our model, we observed that stop gradient makes the training process more stable and allows training the model with a much larger variation of hyperparameters while maintaining stable performance.

Training. Following previous works [8, 10, 13, 23], we use the train set of the ImageNet ILSVRC-2012 dataset [48] for self-supervised training without any human annotation. We train our model with the SGD optimizer [57] with a learning rate of $24.0 \times (\text{batch size}/1024) \times (100/\#epochs)$ and weight decay of 10^{-6} . By default, we use the top $N = 10$ strongest negative examples and an inverse temperature of $\beta = 1$. Due to resource constraints, we train our model with a batch size of 1024 with mixed precision. We use a 10 epoch linear warm-up and a cosine schedule without restarts [34]. Using an 8-GPU (NVIDIA A6000 GPUs) server, training for 100 epochs with $m = 2$ views per image takes approximately 22 hours.

4.2. Evaluation Procedure

Linear Probing. First, we follow the standard protocol and evaluated the learned embedding space by linear evaluation [8, 10, 13, 23], which captures the linear separability of classes in the representation space. For this, we train a linear classifier on frozen representations in a fully-supervised way using the ImageNet train set. We follow the standard protocol [13] to train the linear classifier.

k -NN Evaluation. To analyze local properties of the learned representation, namely how often neighbored data

| Method | Batch Size | Views | Linear Probing (Top-1) | | |
|-------------------|------------|------------------------------|------------------------|--------|--------|
| | | | 100 ep | 200 ep | 400 ep |
| Max-Margin [50] | 256 | 2×224 | 63.8 | - | - |
| MoCo v2† [12] | 256 | 2×224 | 67.4 | 69.9 | 71.0 |
| SimSiam [13] | 256 | 2×224 | 68.1 | 70.0 | 70.8 |
| VICReg [4] | 2048 | 2×224 | 68.6 | - | - |
| Barlow Twins [58] | 2048 | 2×224 | 68.7 | - | - |
| SimCLR† [10] | 4096 | 2×224 | 66.5 | 68.3 | 69.8 |
| SwAV† [8] | 4096 | 2×224 | 66.5 | 69.1 | 70.7 |
| BYOL† [23] | 4096 | 2×224 | 66.5 | 70.6 | 73.2 |
| Whitening [19] | 4096 | 4×224 | 69.4 | - | 72.6 |
| GroCo (ours) | 1024 | 2×224 | 69.2 | 70.4 | 71.0 |
| GroCo (ours) | 1024 | 4×224 | 69.6 | 70.4 | 71.4 |
| SwAV [8] | 4096 | $2 \times 224 + 6 \times 96$ | 72.1 | 73.9 | 74.6 |
| GroCo (ours) | 1024 | $2 \times 224 + 6 \times 96$ | 71.6 | 73.0 | 73.7 |

Table 1. **Comparison with state-of-the-art in linear probing on ImageNet.** We report results for training for 100, 200, and 400 epochs. **Backbone=Resnet50.** †denotes results from SimSiam [13] improved reproductions.

points correspond to the same semantic class, we further evaluate our method by nearest neighbor classification, predicting the object class by a simple weighted k nearest neighbor classifier (k -NN) with $k = \{1, 10, 20\}$ based on cosine distance as in [8, 9]. We again use the ImageNet train set for supervision and test on the ImageNet val set.

4.3. Comparison to State-of-the-Art

We start with a comparison of the proposed method to state-of-the-art self-supervised learning methods in linear probing and k -NN evaluation on the ImageNet [48] and for image retrieval on the revised Oxford and Paris dataset [45].

Linear Probing. In the case of linear probing (Table 1), we observe that our method outperforms almost all baselines in classical (not multi-crop) settings. Our method demonstrates state-of-the-art performance in 100 epochs training, outperforming contrastive baselines SimCLR [10] and MoCo v2 [12] by +2% and information maximization methods Barlow Twins and VICReg by +1% in 100 epochs setup. Moreover, our method outperforms SimCLR and clustering-based SwAV [8] in all other settings as well. Also, we even observe competitive performance compared to BYOL [23] and Whitening [19] methods that use $\times 4$ larger batch size and/or an additional teacher network. We also observe performance improvement by utilizing multiple positive examples during training. In the multi-crop $2 \times 224 + 6 \times 224$ settings, our method is on par with clustering-based SwAV, which utilizes $\times 4$ larger batch size.

k -NN Evaluation. We further evaluate the k -NN performance of our methods compared to multiple state-of-the-art methods with officially released weights in Table 2. We observe that the proposed method excels in all settings, outperforming all methods by more than 4% in the no multi-crop scenario. The method further greatly improves performance by leveraging multiple positive examples. Finally, by uti-

| Method | Batch Size | Views | k -NN (weighted, $k=20$) | | |
|--------------|------------|------------------------------|-----------------------------|--------|--------|
| | | | 100 ep | 200 ep | 400 ep |
| MoCo v2 [12] | 256 | 2×224 | - | 55.6 | - |
| SimSiam [13] | 256 | 2×224 | 57.4 | - | - |
| SimCLR [10] | 4096 | 2×224 | 53.8 | 57.2 | 59.2 |
| SwAV [8] | 4096 | 2×224 | - | - | 61.3 |
| GroCo (ours) | 1024 | 2×224 | 60.5 | 62.7 | 63.6 |
| GroCo (ours) | 1024 | 4×224 | 61.8 | 63.6 | 65.0 |
| SwAV [8] | 4096 | $2 \times 224 + 6 \times 96$ | 61.7 | 63.7 | 64.9 |
| GroCo (ours) | 1024 | $2 \times 224 + 6 \times 96$ | 62.2 | 64.4 | 65.2 |

Table 2. **Comparison with state-of-the-art in k -NN performance on ImageNet.** We evaluate k -NN performance (Top-1) on officially released weights of baseline models trained for 100, 200, and 400 epochs. We used a simple weighted k -NN with $k=20$. **Backbone=Resnet50.**

| Method | Epochs | Batch Size | Views | Oxford | | Paris | |
|--------------|--------|------------|----------------|--------|------|-------|-------|
| | | | | M | H | M | H |
| SimSiam [13] | 100 | 256 | 2×224 | 26.89 | 7.04 | 46.92 | 19.31 |
| MoCo v2 [12] | 200 | 256 | 2×224 | 23.28 | 5.07 | 42.8 | 17.33 |
| SimCLR [10] | 400 | 4096 | 2×224 | 23.27 | 4.56 | 46.93 | 20.19 |
| SwAV [8] | 400 | 4096 | 2×224 | 28.01 | 8.35 | 46.23 | 17.4 |
| GroCo (ours) | 400 | 1024 | 2×224 | 31.77 | 9.08 | 54.79 | 25.77 |

Table 3. **Comparison with state-of-the-art in image retrieval.** We evaluate image retrieval performance on Medium (M) and Hard (H) splits of revisited Oxford and Paris datasets [45]. We evaluate nearest neighbor retrieval performance with ImageNet-trained encoders and report Mean Average Precision.

lizing local-to-global correspondences our method outperforms the SwAV method that uses $\times 4$ larger batch size.

Image Retrieval. To further demonstrate the potential of the proposed methods in nearest neighbors-based tasks, we additionally evaluate ImageNet-trained self-supervised learning methods in image retrieval on the revisited Oxford and Paris datasets [45] in Table 3. We report the Mean Average Precision for the Medium (M) and Hard (H) splits of the datasets as in [9]. We observe that our method outperforms all other methods in this task, confirming its good local properties of learned representations.

4.4. Comparison to the Pairwise Contrastive Loss

To evaluate the properties of the proposed method in a direct comparison with the pairwise contrastive loss formulation, we compared our method to the classical contrastive learning method SimCLR [10], which uses the most popular InfoNCE loss [38] in training. Since SimCLR originally uses only two augmentations per image, we extend it to a group of positives scenario by applying contrastive loss between all possible positive pairs (see supplement). For a fair comparison, we reproduced SimCLR with the 3-layers MLP projection head (as in our method) [11].

Representation Learning Performance. First, we evaluated the learned representations based on the numbers of positive samples in Table 4. We consider four scenarios.

| Method | Views | k -NN Evaluation | | | Linear Eval. | |
|--------------|------------------------------|--------------------|-------------|-------------|--------------|-------------|
| | | $k=1$ | $k=10$ | $k=20$ | Top-1 | Top-5 |
| SimCLR | 2×224 | - | - | - | 64.3 | - |
| SimCLR† | 2×224 | 46.0 | 51.5 | 51.9 | 65.7 | 86.7 |
| SimCLR† | 3×224 | 44.7 | 50.0 | 50.6 | 65.8 | 86.8 |
| SimCLR† | 4×224 | 46.3 | 52.1 | 52.6 | 66.5 | 87.1 |
| SimCLR† | $2 \times 224 + 6 \times 96$ | 46.6 | 51.4 | 52.0 | 67.2 | 87.7 |
| GroCo (ours) | 2×224 | 55.3 | 60.3 | 60.5 | 69.2 | 88.4 |
| GroCo (ours) | 3×224 | 55.8 | 61.2 | 61.6 | 69.5 | 88.8 |
| GroCo (ours) | 4×224 | 56.4 | 61.5 | 61.8 | 69.6 | 88.9 |
| GroCo (ours) | $2 \times 224 + 6 \times 96$ | 57.0 | 61.9 | 62.2 | 71.6 | 90.4 |

Table 4. **Comparison with SimCLR as a contrastive baseline on ImageNet.** Results are reported for k -NN and linear probing. The best results are bolded. **Backbone=Resnet50, #epochs=100, batch size=1024.** †denotes our reproduction.

First, in the 2×224 scenario, we sample only two augmentations per image, and therefore we have only one positive example per data point. In this case, our loss works similarly to SimCLR in a way that it is minimizing the distance between the positive example and the anchor, however, our loss still considers negatives as a group and utilizes only the nearest negative elements that are sorted incorrectly, therefore focusing on local properties of representation space. While outperforming SimCLR baseline by +3% (Top-1) in linear probing, our method also advances in k -NN evaluation by more than +10% ($k=20$), demonstrating that our loss helps to learn better representation not only in terms of linear separability but also in terms of local structure. We further consider settings with 3×224 , 4×224 , and $2 \times 224 + 6 \times 9$ views. We observe that SimCLR shows mixed results from utilizing more views: while it benefits in linear evaluation, performance is not stable in k -NN, for 3×224 performance is lower and for $2 \times 224 + 6 \times 9$ is the same. However, our method clearly profits from utilizing more positives in both evaluations, resulting in +1.7% in k -NN +2.4% in linear evaluation for $2 \times 224 + 6 \times 9$ setup.

Transfer Performance. We further evaluated how well performance transfers on other datasets. In Table 5 we compare Imagenet pre-trained models in k -NN evaluation and linear transfer and on 11 many-shot classification datasets, including FGVC Aircraft [35], Caltech-101 [21], Stanford Cars [31], CIFAR10 [32], CIFAR-100 [32], DTD [14], Oxford 102 Flowers [36], Food-101 [6], Oxford-IIIT Pets [39], SUN397 [53] and Pascal VOC2007 [20]. For linear transfer evaluation, we follow the experimental protocol provided in [18] without any modification. We observe that the proposed method is on par with SimCLR in linear evaluation. In zero-shot k -NN evaluation, our method excels in 10 out of 11 datasets, in particular improving performance on the Pets dataset by +15%, and on the Aircraft and Food datasets by +4%. This shows that the improved k -NN performance transfers to downstream tasks as well.

| Method | Evaluation | Aircraft | Caltech101 | Cars | Cifar10 | Cifar100 | DTD | Flowers | Food | Pets | SUN397 | VOC2007 | Average |
|--------------|-----------------------------|--------------|--------------|--------------|--------------|--------------|--------------|--------------|--------------|--------------|--------------|--------------|--------------|
| SimCLR† | k -NN (weighted, $k=20$) | 19.5 | 75.8 | 15.2 | 85.1 | 63.3 | 70.9 | 73.1 | 47.9 | 60.6 | 46.3 | 70.0 | 57.06 |
| GroCo (ours) | k -NN (weighted, $k=20$) | 23.7 | 79.3 | 17.5 | 85.4 | 63.6 | 69.3 | 77.7 | 52.8 | 75.9 | 50.1 | 73.7 | 60.81 |
| SimCLR† | Linear transfer | 42.51 | 85.10 | 43.19 | 90.86 | 74.54 | 75.11 | 91.59 | 68.20 | 77.92 | 58.43 | 78.74 | 71.47 |
| GroCo (ours) | Linear transfer | 45.90 | 86.44 | 42.63 | 89.26 | 70.72 | 72.77 | 88.41 | 66.72 | 84.29 | 58.51 | 81.34 | 71.55 |

Table 5. **Comparison with SimCLR as a contrastive baseline in transfer performance on 11 classification datasets.** Models are pre-trained on Imagenet. **Backbone=Resnet50, #epochs=100, batch size=1024, views=2x224.** †denotes our reproduction.

| | k -NN Evaluation | | | Linear Probing | |
|-----------------------------------|--------------------|-------------|-------------|----------------|-------------|
| | $k=1$ | $k=10$ | $k=20$ | Top-1 | Top-5 |
| Triplet Loss (margin=0.8) | 46.8 | 52.5 | 52.8 | 63.9 | 85.4 |
| Triplet Loss (margin=1.6) | 47.9 | 53.4 | 53.7 | 64.2 | 85.3 |
| Triplet Loss (margin= $+\infty$) | 47.9 | 53.3 | 53.8 | 64.3 | 85.3 |
| GroCo (Ours) | 54.7 | 59.5 | 60.0 | 68.5 | 88.2 |

(a) Ordering supervision.

| | k -NN Evaluation | | | Linear Probing | |
|--------------------|--------------------|-------------|-------------|----------------|-------------|
| | $k=1$ | $k=10$ | $k=20$ | Top-1 | Top-5 |
| Randomly ordered | 54.1 | 59.2 | 59.4 | 68.4 | 88.2 |
| Pre-ordered (Ours) | 54.7 | 59.5 | 60.0 | 68.5 | 88.2 |

(b) Pre-ordering in the groups.

| Inverse temp. β | Number of negatives N | | | | | |
|--------------------------|-------------------------|--------|-------------|-------------|---------|--------|
| | 5 | | 10 | | 20 | |
| | k -NN | Lin.p. | k -NN | Lin.p. | k -NN | Lin.p. |
| 0.25 | 58.9 | 67.9 | - | - | - | - |
| 0.5 | 59.1 | 67.5 | 59.8 | 68.5 | - | - |
| 1 | 58.8 | 67.7 | 60.0 | 68.5 | 54.4 | 65.2 |
| 2 | - | - | 60.0 | 68.3 | 56.2 | 65.7 |
| 4 | - | - | - | - | 59.2 | 67.7 |
| 8 | - | - | - | - | 58.6 | 67.7 |

(c) An inverse temperature β , a number of negatives N .

| Batch Size | k -NN Evaluation | | | Linear Probing | |
|------------|--------------------|-------------|-------------|----------------|-------------|
| | $k=1$ | $k=10$ | $k=20$ | Top-1 | Top-5 |
| 256 | 52.2 | 56.8 | 56.8 | 67.2 | 87.7 |
| 512 | 53.1 | 57.9 | 58.1 | 67.7 | 87.8 |
| 1024 | 54.7 | 59.5 | 60.0 | 68.5 | 88.2 |

(d) Batch size.

Table 6. **Ablation Experiments.** For (c), we report k -NN performance with $k=20$, and linear probing performance (Top-1), denoted as Lin.p. The best results are bolded. Options used to obtain the main results are highlighted. **Backbone=Resnet50, Views=2x224, #epochs=100, Weight Decay=0.5e-6.**

4.5. Ablation Study

Finally, we analyze the design choices of our method.

Ordering Supervision. First, we compare the group ordering supervision via differentiable sorting with a triplet loss formulation $L = \max(d_i^p - d_j^n + r, 0)$, where r is a margin. For a fair comparison, we consider all positive and the 10 strongest negative samples and evaluate different margin parameters in Table 6a. Here, sorting is superior to a triplet loss with hard margin selection.

Pre-ordering in Groups. We analyze the impact of pre-

ordering elements within the negative and positive groups before forwarding them to the sorting network in Table 6b. We observe that our methods achieve competitive performance even without pre-ordering; however, pre-ordering strengthens our method further.

Inverse Temperature, Number of Negatives. In Table 6c, we examine the influence of the number of nearest neighbor negatives N used in the loss, as well as the value of the inverse temperature parameter β (Equation 2). We observe that usage of too many negatives may not be beneficial for the model. Since our loss focuses on negatives that are sorted incorrectly, increasing the number of negatives at some point does not bring any new learning signal (because more distant is unlikely to be sorted incorrectly). However, a larger N results in more steps of the sorting network, increasing the degree of relaxation. Using a larger inverse temperature β (leading to a lower degree of relaxation in the swap operation) we can gain some performance; however, the variance of the gradients is larger with a larger β , which is not beneficial for optimization. We found that $N = 10$ and $\beta = 1$ is the most efficient configuration.

Batch Size. The large batch size might be an important factor in obtaining good performance for many self-supervised learning methods. We find that our method is quite robust for training with smaller batch sizes (Table 6d).

Training Time. We also consider the training time of our model compared to SimCLR baseline. To eliminate the influence of distributed training, we measure the average time of training iteration on one GPU. We find that the iteration time of both models is comparable, 514ms for SimCLR vs 526ms for the proposed methods for a batch size of 128.

5. Conclusion

In this paper, we proposed an alternative approach to the common pairwise contrastive learning formulation. Namely, we proposed the group ordering constraints, that consider positives and negatives as groups and enforce the group of positives to be closer to the anchor image than the negative group. To enforce these constraints, we leveraged recent progress in the context of differentiable sorting approaches and formulated a group ordering loss based on the given sorting supervision. Our evaluation showed that the proposed framework, does not only compete with current contrastive loss baselines, but actually outperforms standard contrastive learning with regards to all k -NN-based metrics.

References

- [1] Hassan Akbari, Liangzhe Yuan, Rui Qian, Wei-Hong Chuang, Shih-Fu Chang, Yin Cui, and Boqing Gong. Vatt: Transformers for multimodal self-supervised learning from raw video, audio and text. *NeurIPS*, 34:24206–24221, 2021. [3](#)
- [2] Yuki Markus Asano, Christian Rupprecht, and Andrea Vedaldi. Self-labelling via simultaneous clustering and representation learning. *arXiv preprint arXiv:1911.05371*, 2019. [3](#)
- [3] Philip Bachman, R Devon Hjelm, and William Buchwalter. Learning representations by maximizing mutual information across views. *NeurIPS*, 32, 2019. [1](#)
- [4] Adrien Bardes, Jean Ponce, and Yann LeCun. Vircreg: Variance-invariance-covariance regularization for self-supervised learning. *arXiv preprint arXiv:2105.04906*, 2021. [1](#), [3](#), [6](#)
- [5] Mathieu Blondel, Olivier Teboul, Quentin Berthet, and Josip Djolonga. Fast Differentiable Sorting and Ranking. In *ICML*, 2020. [3](#)
- [6] Lukas Bossard, Matthieu Guillaumin, and Luc Van Gool. Food-101—mining discriminative components with random forests. In *ECCV*, pages 446–461. Springer, 2014. [7](#)
- [7] Mathilde Caron, Piotr Bojanowski, Armand Joulin, and Matthijs Douze. Deep clustering for unsupervised learning of visual features. In *ECCV*, pages 132–149, 2018. [3](#)
- [8] Mathilde Caron, Ishan Misra, Julien Mairal, Priya Goyal, Piotr Bojanowski, and Armand Joulin. Unsupervised learning of visual features by contrasting cluster assignments. *NeurIPS*, 33:9912–9924, 2020. [1](#), [3](#), [6](#), [7](#), [13](#)
- [9] Mathilde Caron, Hugo Touvron, Ishan Misra, Hervé Jégou, Julien Mairal, Piotr Bojanowski, and Armand Joulin. Emerging properties in self-supervised vision transformers. In *ICCV*, pages 9650–9660, 2021. [1](#), [3](#), [6](#), [7](#), [11](#), [12](#), [13](#)
- [10] Ting Chen, Simon Kornblith, Mohammad Norouzi, and Geoffrey Hinton. A simple framework for contrastive learning of visual representations. In *ICML*, pages 1597–1607. PMLR, 2020. [1](#), [3](#), [6](#), [7](#), [11](#), [13](#)
- [11] Ting Chen, Simon Kornblith, Kevin Swersky, Mohammad Norouzi, and Geoffrey E Hinton. Big self-supervised models are strong semi-supervised learners. *NeurIPS*, 33:22243–22255, 2020. [3](#), [7](#)
- [12] Xinlei Chen, Haoqi Fan, Ross Girshick, and Kaiming He. Improved baselines with momentum contrastive learning. *arXiv preprint arXiv:2003.04297*, 2020. [3](#), [6](#), [7](#)
- [13] Xinlei Chen and Kaiming He. Exploring simple siamese representation learning. In *CVPR*, pages 15750–15758, 2021. [1](#), [3](#), [6](#), [7](#), [13](#)
- [14] Mircea Cimpoi, Subhransu Maji, Iasonas Kokkinos, Sammy Mohamed, and Andrea Vedaldi. Describing textures in the wild. In *CVPR*, pages 3606–3613, 2014. [7](#)
- [15] Jean-Baptiste Cordonnier, Aravindh Mahendran, Alexey Dosovitskiy, Dirk Weissenborn, Jakob Uszkoreit, and Thomas Unterthiner. Differentiable patch selection for image recognition. In *CVPR*, pages 2351–2360, 2021. [3](#)
- [16] Marco Cuturi, Olivier Teboul, and Jean-Philippe Vert. Differentiable ranking and sorting using optimal transport. *NeurIPS*, 32, 2019. [2](#), [3](#)
- [17] Debidatta Dwibedi, Yusuf Aytar, Jonathan Tompson, Pierre Sermanet, and Andrew Zisserman. With a little help from my friends: Nearest-neighbor contrastive learning of visual representations. In *ICCV*, pages 9588–9597, 2021. [1](#), [3](#)
- [18] Linus Ericsson, Henry Gouk, and Timothy M Hospedales. How well do self-supervised models transfer? In *CVPR*, pages 5414–5423, 2021. [7](#)
- [19] Aleksandr Ermolov, Aliaksandr Siarohin, Enver Sangineto, and Nicu Sebe. Whitening for self-supervised representation learning. In *ICML*, pages 3015–3024. PMLR, 2021. [1](#), [3](#), [6](#)
- [20] Mark Everingham, Luc Van Gool, Christopher KI Williams, John Winn, and Andrew Zisserman. The pascal visual object classes (voc) challenge. *IJCV*, 88(2):303–338, 2010. [7](#)
- [21] Li Fei-Fei, Rob Fergus, and Pietro Perona. Learning generative visual models from few training examples: An incremental bayesian approach tested on 101 object categories. In *CVPR*, pages 178–178. IEEE, 2004. [7](#)
- [22] Spyros Gidaris, Praveer Singh, and Nikos Komodakis. Unsupervised representation learning by predicting image rotations. *arXiv preprint arXiv:1803.07728*, 2018. [3](#)
- [23] Jean-Bastien Grill, Florian Strub, Florent Altché, Corentin Tallec, Pierre Richemond, Elena Buchatskaya, Carl Doersch, Bernardo Avila Pires, Zhaohan Guo, Mohammad Gheshlaghi Azar, et al. Bootstrap your own latent—a new approach to self-supervised learning. *NeurIPS*, 33:21271–21284, 2020. [1](#), [3](#), [6](#)
- [24] Aditya Grover, Eric Wang, Aaron Zweig, and Stefano Ermon. Stochastic Optimization of Sorting Networks via Continuous Relaxations. In *ICLR*, 2019. [2](#), [3](#)
- [25] Hussein Hazimeh, Zhe Zhao, Aakanksha Chowdhery, Maheswaran Sathiamoorthy, Yihua Chen, Rahul Mazumder, Lichan Hong, and Ed Chi. Dselect-k: Differentiable selection in the mixture of experts with applications to multi-task learning. *NeurIPS*, 34, 2021. [3](#)
- [26] Kaiming He, Haoqi Fan, Yuxin Wu, Saining Xie, and Ross Girshick. Momentum contrast for unsupervised visual representation learning. *CVPR*, 2012. [1](#), [3](#)
- [27] Kaiming He, Xiangyu Zhang, Shaoqing Ren, and Jian Sun. Deep residual learning for image recognition. In *CVPR*, pages 770–778, 2016. [6](#)
- [28] Tri Huynh, Simon Kornblith, Matthew R Walter, Michael Maire, and Maryam Khademi. Boosting contrastive self-supervised learning with false negative cancellation. In *Proceedings of the IEEE/CVF Winter Conference on Applications of Computer Vision*, pages 2785–2795, 2022. [3](#)
- [29] Sergey Ioffe and Christian Szegedy. Batch normalization: Accelerating deep network training by reducing internal covariate shift. In *ICML*, pages 448–456. PMLR, 2015. [6](#)
- [30] Donald E. Knuth. *The Art of Computer Programming, Volume 3: Sorting and Searching (2nd Ed.)*. Addison Wesley, 1998. [4](#), [13](#)
- [31] Jonathan Krause, Jia Deng, Michael Stark, and Li Fei-Fei. Collecting a large-scale dataset of fine-grained cars. *Second Workshop on Fine-Grained Visual Categorization*, 2013. [7](#)

- [32] Alex Krizhevsky, Geoffrey Hinton, et al. Learning multiple layers of features from tiny images. *Technical Report*, 2009. 7
- [33] Hyunsung Lee, Sangwoo Cho, Yeongjae Jang, Jaekwang Kim, and Honguk Woo. Differentiable ranking metric using relaxed sorting for top-k recommendation. *IEEE Access*, 9:114649–114658, 2021. 3
- [34] Ilya Loshchilov and Frank Hutter. Sgdr: Stochastic gradient descent with warm restarts. *arXiv preprint arXiv:1608.03983*, 2016. 6
- [35] Subhransu Maji, Esa Rahtu, Juho Kannala, Matthew Blaschko, and Andrea Vedaldi. Fine-grained visual classification of aircraft. *arXiv preprint arXiv:1306.5151*, 2013. 7
- [36] Maria-Elena Nilsback and Andrew Zisserman. Automated flower classification over a large number of classes. In *2008 Sixth Indian Conference on Computer Vision, Graphics & Image Processing*, pages 722–729. IEEE, 2008. 7
- [37] Mehdi Noroozi and Paolo Favaro. Unsupervised learning of visual representations by solving jigsaw puzzles. In *ECCV*, pages 69–84. Springer, 2016. 3
- [38] Aaron van den Oord, Yazhe Li, and Oriol Vinyals. Representation learning with contrastive predictive coding. *arXiv preprint arXiv:1807.03748*, 2018. 7
- [39] Omkar M Parkhi, Andrea Vedaldi, Andrew Zisserman, and CV Jawahar. Cats and dogs. In *CVPR*, pages 3498–3505. IEEE, 2012. 7
- [40] Deepak Pathak, Philipp Krahenbuhl, Jeff Donahue, Trevor Darrell, and Alexei A Efros. Context encoders: Feature learning by inpainting. In *CVPR*, pages 2536–2544, 2016. 3
- [41] Felix Petersen, Christian Borgelt, Hilde Kuehne, and Oliver Deussen. Differentiable Sorting Networks for Scalable Sorting and Ranking Supervision. In *ICML*, 2021. 2, 3, 4
- [42] Felix Petersen, Christian Borgelt, Hilde Kuehne, and Oliver Deussen. Monotonic differentiable sorting networks. *ICLR*, 2022. 2, 3, 4
- [43] Felix Petersen, Hilde Kuehne, Christian Borgelt, and Oliver Deussen. Differentiable top-k classification learning. In *ICML*, pages 17656–17668. PMLR, 2022. 5
- [44] Sebastian Prillo and Julian Eisenschlos. Softsort: A continuous relaxation for the argsort operator. In *ICML*, pages 7793–7802. PMLR, 2020. 3
- [45] Filip Radenović, Ahmet Iscen, Giorgos Tolias, Yannis Avrithis, and Ondřej Chum. Revisiting oxford and paris: Large-scale image retrieval benchmarking. In *CVPR*, pages 5706–5715, 2018. 6, 7
- [46] Alec Radford, Jong Wook Kim, Chris Hallacy, Aditya Ramesh, Gabriel Goh, Sandhini Agarwal, Girish Sastry, Amanda Askell, Pamela Mishkin, Jack Clark, et al. Learning transferable visual models from natural language supervision. In *ICML*, pages 8748–8763. PMLR, 2021. 3
- [47] Joshua Robinson, Ching-Yao Chuang, Suvrit Sra, and Stefanie Jegelka. Contrastive learning with hard negative samples. *arXiv preprint arXiv:2010.04592*, 2020. 2, 3, 12
- [48] Olga Russakovsky, Jia Deng, Hao Su, Jonathan Krause, Sanjeev Satheesh, Sean Ma, Zhiheng Huang, Andrej Karpathy, Aditya Khosla, Michael Bernstein, et al. Imagenet large scale visual recognition challenge. *IJCV*, 115(3):211–252, 2015. 6
- [49] Florian Schroff, Dmitry Kalenichenko, and James Philbin. Facenet: A unified embedding for face recognition and clustering. In *CVPR*, pages 815–823, 2015. 3, 11
- [50] Anshul Shah, Suvrit Sra, Rama Chellappa, and Anoop Cherian. Max-margin contrastive learning. In *Proceedings of the AAAI Conference on Artificial Intelligence*, 2022. 2, 6
- [51] Yonglong Tian, Chen Sun, Ben Poole, Dilip Krishnan, Cordelia Schmid, and Phillip Isola. What makes for good views for contrastive learning? *NeurIPS*, 33:6827–6839, 2020. 1
- [52] Chao-Yuan Wu, R Manmatha, Alexander J Smola, and Philipp Krahenbuhl. Sampling matters in deep embedding learning. In *ICCV*, pages 2840–2848, 2017. 1
- [53] Jianxiong Xiao, James Hays, Krista A Ehinger, Aude Oliva, and Antonio Torralba. Sun database: Large-scale scene recognition from abbey to zoo. In *CVPR*, pages 3485–3492. IEEE, 2010. 7
- [54] Tete Xiao, Xiaolong Wang, Alexei A Efros, and Trevor Darrell. What should not be contrastive in contrastive learning. *arXiv preprint arXiv:2008.05659*, 2020. 3
- [55] Hong Xuan, Abby Stylianou, Xiaotong Liu, and Robert Pless. Hard negative examples are hard, but useful. In *ECCV*, pages 126–142. Springer, 2020. 11
- [56] Mang Ye, Xu Zhang, Pong C Yuen, and Shih-Fu Chang. Unsupervised embedding learning via invariant and spreading instance feature. In *CVPR*, pages 6210–6219, 2019. 1
- [57] Yang You, Igor Gitman, and Boris Ginsburg. Large batch training of convolutional networks. *arXiv preprint arXiv:1708.03888*, 2017. 6, 13
- [58] Jure Zbontar, Li Jing, Ishan Misra, Yann LeCun, and Stéphane Deny. Barlow twins: Self-supervised learning via redundancy reduction. In *ICML*, pages 12310–12320. PMLR, 2021. 1, 3, 6
- [59] Fangneng Zhan, Yingchen Yu, Rongliang Wu, Kaiwen Cui, Aoran Xiao, Shijian Lu, and Ling Shao. Bi-level feature alignment for versatile image translation and manipulation. *arXiv preprint arXiv:2107.03021*, 2021. 3
- [60] Richard Zhang, Phillip Isola, and Alexei A Efros. Colorful image colorization. In *ECCV*, pages 649–666. Springer, 2016. 3

Supplementary Material

In the supplementary material, we first discuss relations between the GroCo loss, the contrastive loss, and the triplet loss in Section A. Then we provide additional experimental evaluation results in Section B and qualitative analysis in Section C. Then we describe odd-even sorting networks in Section D. Finally, we cover additional implementation details in Section E.

A. Discussion of GroCo/Contrastive/Triplet Loss Relations

In this section, we discuss the similarities and differences between the GroCo loss, the contrastive loss, and the triplet loss. For comparison purposes, let's consider a simplified version of losses when there is only one positive example x^p and one negative example x^n for the anchor x^a . We denote the distance from the anchor x^a to the positive sample x^p as $d^p = -\frac{x^a \top x^p}{\|x^a\| \|x^p\|}$ and the distance from the anchor x^a to the negative sample x^n as $d^n = -\frac{x^a \top x^n}{\|x^a\| \|x^n\|}$. Then contrastive InfoNCE loss (with respect to the anchor x^a) is defined as:

$$L_{Contrastive} = -\log \frac{\exp(-d^p/\tau)}{\exp(-d^p/\tau) + \exp(-d^n/\tau)} \quad (6)$$

$$= \log(1 + \exp(-(d^n - d^p)/\tau)),$$

where τ is a temperature hyperparameter (Figure 4a).

The triplet loss is defined as:

$$L_{Triplet} = \max(d^p - d^n + r, 0) = \max(r - (d^n - d^p), 0), \quad (7)$$

where r is a margin hyperparameter (Figure 4b).

For the GroCo loss, a permutation matrix $P \in R^{2 \times 2}$ corresponds to only one conditional swap operation and is defined as:

$$P_{11} = P_{22} = f(d^n - d^p) = \frac{1}{\pi} \arctan(\beta(d^n - d^p)) + 0.5,$$

$$P_{12} = P_{21} = f(d^p - d^n) = \frac{1}{\pi} \arctan(\beta(d^p - d^n)) + 0.5, \quad (8)$$

where β is an inverse temperature. Therefore, the GroCo loss is defined as:

$$L_{GroCo} = \frac{1}{4} \left(-2 \log \left(\frac{1}{\pi} \arctan(\beta(d^n - d^p)) + 0.5 \right) - \right.$$

$$\left. -2 \log \left(1 - \frac{1}{\pi} \arctan(\beta(d^p - d^n)) - 0.5 \right) \right) =$$

$$= -\log \left(\frac{1}{\pi} \arctan(\beta(d^n - d^p)) + 0.5 \right), \quad (9)$$

where β is an inverse temperature hyperparameter (Figure 4c).

In Figure 4, we show the loss curves with different values of respective hyperparameters. We note that in this simplified example with only one positive and only one negative, all three losses try to maximize the difference between the distances to the positive and negative examples ($d^n - d^p$). The temperature τ , the margin r , or the inverse temperature β define the flatness of the loss curve depending on the difference ($d^n - d^p$).

However, in the case with more negative/positive examples for the anchor image, different losses integrate information from multiple negatives/positives in different ways. For triplet loss, there are various strategies to sample one positive example and one negative example for the anchor image [49, 55]. The complete loss is defined as the sum (or average) of the losses for the chosen triplets $\sum_{ij} \max(r - (d_i^n - d_j^p), 0)$. On the other hand, the contrastive loss aggregates multiple negatives by contrasting the positive example to all negative examples, resulting in sum under logarithm: $\log(1 + \sum_i \exp(-(d_i^n - d^p)/\tau))$. And in contrast to an explicit sum over a predefined number of negatives, the GroCo loss aggregates multiple positives and negatives via the permutation matrix, conditionally swapping neighboring elements, and later applies the group ordering supervision, enforcing the distance between positive and negative groups.

B. Additional Experimental Results

In this section, we provide additional experimental evaluations:

Augmentation Strategy. In Table 7a we evaluate the performance of the model with respect to different augmentation strategies for view sampling. We follow two setups: 1) the augmentation strategy as used in the SimCLR [10] method with a random resized crop, color jittering, and gaussian blur, grayscaling and horizontal flip and 2) the augmentation strategy as used in the DINO [9] method that extends the SimCLR list of augmentations with solarization. SimCLR augmentations are considered as “stronger” compared to DINO augmentations since they include a larger range of cropping sizes (8% -100% of original image compared to 14%-100% in DINO augmentations) and larger range values in color jittering. We observe that the stronger SimCLR [10] augmentations are more beneficial for the SimCLR method than the weaker DINO augmentations, while for the proposed method, the DINO augmentation strategy is more beneficial. However, the difference between augmentation strategies diminishes with increasing number of training epochs and is no longer measurable at 400 epochs. For a fair comparison, we use the SimCLR augmentation strategy in all reproductions of the SimCLR method reported in the main paper.

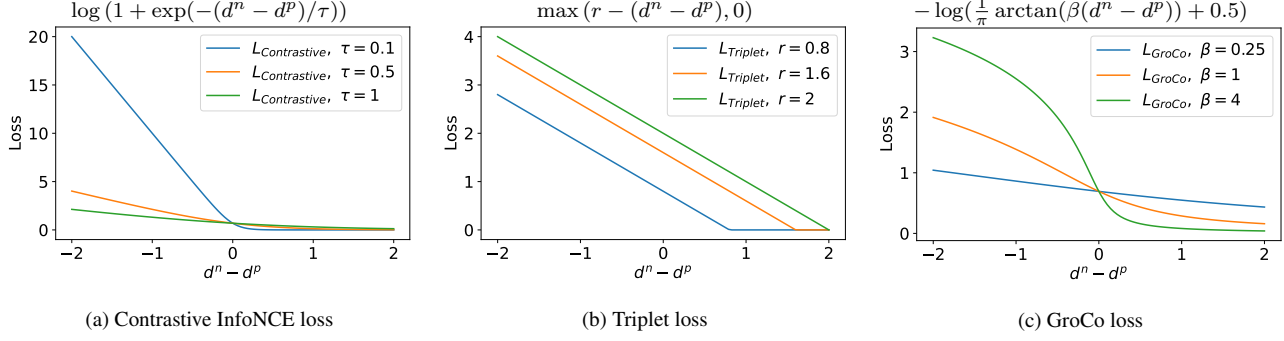


Figure 4. Comparison of the contrastive loss, the triplet loss, and the GroCo loss in a simple scenario with only one positive example and one negative example for an anchor image. We denote the distance from the anchor to the positive sample as d^p and the distance from the anchor to the negative sample as d^n . We note that in the simple case of only one positive and one negative, all three losses try to maximize the difference between the distances to the positive and negative examples ($d^n - d^p$). The temperature τ , the margin r , or the inverse temperature β define the flatness of the loss curve depending on the difference ($d^n - d^p$).

| Method | Augmentations | Epochs | k -NN Evaluation | | | Linear Evaluation | |
|--------|------------------|--------|--------------------|-------------|-------------|-------------------|-------------|
| | | | $k=1$ | $k=10$ | $k=20$ | Top-1 | Top-5 |
| SimCLR | as in SimCLR [9] | 100 | 46.0 | 51.5 | 51.9 | 65.7 | 86.7 |
| SimCLR | as in DINO [9] | 100 | 43.3 | 48.6 | 49.1 | 63.7 | 85.4 |
| GroCo | as in SimCLR [9] | 100 | 54.0 | 59.0 | 59.4 | 68.4 | 88.3 |
| GroCo | as in DINO [9] | 100 | 55.3 | 60.3 | 60.5 | 69.2 | 88.4 |
| GroCo | as in SimCLR [9] | 200 | 56.7 | 61.6 | 61.8 | 69.8 | 89.1 |
| GroCo | as in DINO [9] | 200 | 57.7 | 62.4 | 62.7 | 70.4 | 89.5 |
| GroCo | as in SimCLR [9] | 400 | 58.3 | 63.3 | 63.8 | 71.1 | 89.7 |
| GroCo | as in DINO [9] | 400 | 58.7 | 63.4 | 63.6 | 71.0 | 89.7 |

(a) Augmentation strategy

| Projection dim | Embedding dim | k -NN Evaluation | | | Linear Probing | |
|----------------|---------------|--------------------|-------------|-------------|----------------|-------------|
| | | $k=1$ | $k=10$ | $k=20$ | Top-1 | Top-5 |
| 128 | 2048 | 53.7 | 58.5 | 58.7 | 68.1 | 88.0 |
| 512 | 2048 | 55.2 | 59.8 | 60.1 | 69.0 | 88.5 |
| 2048 | 2048 | 55.3 | 60.3 | 60.5 | 69.2 | 88.4 |

(b) Projection dimensionality

| | k -NN Evaluation | | | Linear Probing | |
|----------------------------|--------------------|-------------|-------------|----------------|-------------|
| | $k=1$ | $k=10$ | $k=20$ | Top-1 | Top-5 |
| 10 random negatives | 39.5 | 45.0 | 45.3 | 60.1 | 82.7 |
| top-10 strongest negatives | 55.3 | 60.3 | 60.5 | 69.2 | 88.4 |

(c) Importance of negatives

| Method | Space | k -NN Evaluation | | |
|--------|----------------------|--------------------|-------------|-------------|
| | | $k=1$ | $k=10$ | $k=20$ |
| SimCLR | Projection Space | 35.8 | 41.6 | 42.3 |
| SimCLR | Representation Space | 46.0 | 51.5 | 51.9 |
| GroCo | Projection Space | 51.4 | 56.9 | 57.3 |
| GroCo | Representation Space | 55.3 | 60.3 | 60.5 |

(d) k -NN evaluation

Table 7. **Additional Experiments.** The best results are bolded. Options used to obtain the main results are highlighted. **Backbone=Resnet50, Views=2×224, #epochs=100.**

Projection Dimensionality. We also ablate our method with respect to the dimensionality of the projection space

(or the latent space), where distances between samples are computed to calculate a training loss. Table 7b shows that increasing dimensionality of the projection space increases performance in general, which is more noticeable for the k -NN performance. Note that we do not change the dimensionality of the embedding space (output space of the encoder that is used for the k -NN evaluation and linear evaluation), which is always 2048-dimensional.

Importance of Negatives. We also evaluate the importance of utilizing strong negatives for the successful training of our model. We train the model using ten random negatives instead of the top-10 strongest negatives as a negative group and report performance in Table 7c. We observe that leveraging the strongest negatives increases performance across all metrics, demonstrating the importance of hard negatives during training with the GroCo loss, similarly as the contrastive loss benefits from hard negative sampling [47].

k -NN in Projection Space. We also evaluate the k -NN performance in the projection space (or the latent space) where the training loss is applied. We compare k -NN performance in the projection and representation spaces in Table 7d. We observe that for both methods, k -NN performance is higher if we use embeddings from the representation space even though we train the model to compare embeddings in the projection space. This could be explained by the fact that the embedding space contains more general image representations since the representations in projection space could be overfitted to the respective augmentations and there become agnostic to some image attributes (like color, since we train the model to match views with different color jittering parameters).

Algorithm 1 Python pseudocode of an odd-even sorting network for sorting an array of numbers in non-descending order

```
# arr: array to sort
# n: length of array

for s in range(1, n + 1):
    if s % 2 == 1:
        for i in range(0, n - 1, 2):
            if arr[i] > arr[i+1]:
                arr[i], arr[i+1] = arr[i+1], arr[i]
    else:
        for i in range(1, n - 1, 2):
            if arr[i] > arr[i+1]:
                arr[i], arr[i+1] = arr[i+1], arr[i]
```

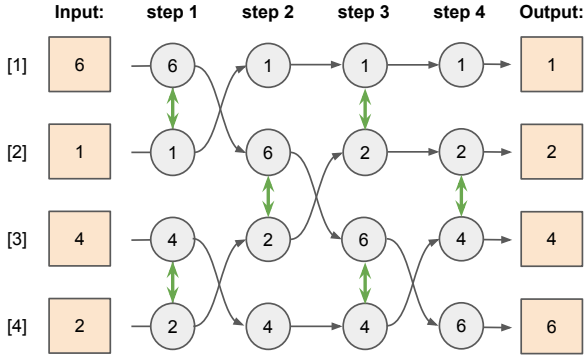


Figure 5. An illustration of an odd-even sorting network for sorting four elements in non-descending order with an example of sorting of [6, 1, 4, 2] array.

C. Qualitative Analysis of Learned Representation Space

We also additionally perform a qualitative analysis of learned representation. In Figure 6, we visualize representations for images from four classes of different types of cats and four classes of different types of dogs. We find that our method produces much more visually separable clusters with respect to “inter-class” variations (cats vs dogs) and “intra-class” variations (between different classes of cats) than the SimCLR baseline.

D. Odd-even Sorting Network

An odd-even sorting network, or odd-even sort, is a sorting algorithm from classic computer science literature [30]. Sorting networks, or networks for sorting, are a family of sorting algorithms that consist of the *fixed* sequence of comparisons, in a sense that the next comparisons (elements on which positions are compared) does not depend on the result of previous comparisons. An odd-even sorting network is a simple example of this family of algorithms. The odd-even sorting network compares neighbored elements starting from odd and even indices alternating on each step, and requires n steps to sort a sequence of n elements. We

present a pseudocode of the odd-even sorting network in Algorithm 1. We also additionally illustrate the odd-even sorting process in Figure 5.

E. Implementation Details

E.1. Linear Evaluation Details

For linear evaluation, we train a linear classifier on frozen representations in a fully-supervised way, using the training set of ImageNet for training and the validation set for evaluation. We follow the training protocol of SimCLR [10] and SimSiam [13] and train a linear classifier for 90 epochs using the LARS optimizer [57] with the batch size of 4096, the momentum of 0.9, the linear rate of 1.6 (following the rule: learning rate = $0.1 \times \text{batch size}/256$), without a warmup and weight decay. Following [10] and [13], we use weak data augmentation (only random cropping with horizontal flipping) and apply gradient stopping on the input of the classifier to prevent updating the encoder.

E.2. SimCLR with Multiple Positives

To train SimCLR with more than one positive view per anchor, we apply contrastive loss for all possible positive pairs, considering all views from other images in the batch as negatives (with a batch of B examples with have $m(B - 1)$ negatives views). Let x_i^b denote the i ’th view of the b ’th image in a batch, and $P_{x_i^b}$ denote a set of positive samples for the anchor x_i^b , and $N_{x_i^b}$ denote a set of positive samples for the anchor x_i^b . Then, the loss is calculated as

$$\mathcal{L}_{\text{SimCLR}} = \frac{1}{B} \sum_{b=1}^B \frac{1}{m} \sum_{i=1}^m \frac{1}{\|P_{x_i^b}\|} \sum_{y \in P_{x_i^b}} -\log \left(\frac{\exp(-d(x_i^b, y)/\tau)}{\exp(-d(x_i^b, y)/\tau) + \sum_{z \in N_{x_i^b}} \exp(-d(x_i^b, z)/\tau)} \right), \quad (10)$$

where τ is a temperature parameter. This extension of the SimCLR framework for $m > 2$ views per image is the same as used in the SwAV evaluations [8]. Note that in the multi-crop scenario, we use only full-resolution global views as positive examples following “local-global” correspondence idea [8, 9].

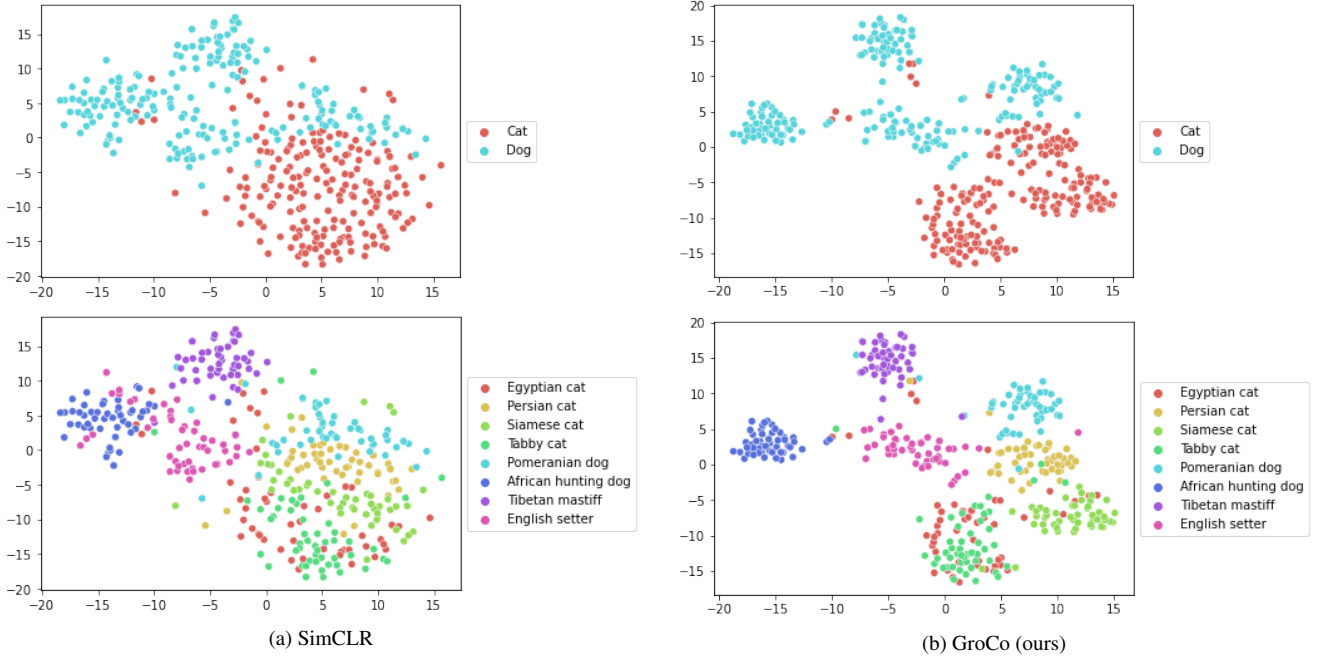


Figure 6. t-SNE visualization of learned representations of Imagenet validation images from four classes of different types of cats (Egyptian cat, Persian cat, Siamese cat, Tabby cat) and four classes different types of dogs (Pomeranian dog, African hunting dog, Tibetan mastiff, English setter) for the SimCLR method and the proposed method. For visualization we use models with Resnet50 encoder trained for 100 epochs with a batch size of 1024 and 2×224 views.